CORTEX 123 (2020) 185–199

Available online at www.sciencedirect.com

ScienceDirect

Journal homepage: www.elsevier.com/locate/cortex

Research Report

Functional connectivity of the orbitofrontal cortex, anterior cingulate cortex, and inferior frontal gyrus in humans

Jingnan Du [a,b,1], Edmund T. Rolls [a,c,d,1], Wei Cheng [a,b,*], Yu Li [e,1], Weikang Gong [a], Jiang Qiu [e] and Jianfeng Feng [a,b,c,**]

[a] Institute of Science and Technology for Brain-inspired Intelligence, Fudan University, Shanghai, PR China
[b] Key Laboratory of Computational Neuroscience, Institute of Science and Technology for Brain-inspired Intelligence, Fudan University, Ministry of Education, PR China
[c] Department of Computer Science, University of Warwick, Coventry, UK
[d] Oxford Centre for Computational Neuroscience, Oxford, UK
[e] Key Laboratory of Cognition and Personality (SWU), Ministry of Education, Chongqing, China

ARTICLE INFO

Article history:
Received 4 July 2019
Reviewed 26 August 2019
Revised 2 September 2019
Accepted 2 October 2019
Action editor Stefano Cappa
Published online 16 November 2019

Keywords:
Orbitofrontal cortex
Anterior cingulate cortex
Inferior frontal gyrus
Parcellation
Functional connectivity

ABSTRACT

Parcellation of the orbitofrontal cortex, anterior cingulate cortex, and inferior frontal gyrus based on their functional connectivity with the whole brain in resting state fMRI with 654 participants was performed to investigate how these regions with different functions in reward, emotion and their disorders are functionally connected to each other and to the whole brain. The human medial and lateral orbitofrontal cortex, the ventromedial prefrontal cortex, the anterior cingulate cortex, and the right and left inferior frontal gyrus have different functional connectivity with other brain areas and with each other; and each of these regions has several parcels with different functional connectivity with other brain areas. In terms of functional connectivity, the lateral orbitofrontal cortex extends especially on the right into the orbital part of the inferior frontal gyrus and provides connectivity with premotor cortical areas. The orbitofrontal cortex, especially the lateral orbitofrontal cortex, has connectivity not only with language-related areas in the inferior frontal gyrus (Broca's area), but also with the angular and supramarginal gyri. In this context, whereas the connectivity of the orbitofrontal cortex, ventromedial prefrontal cortex, and anterior cingulate cortex is symmetrical, the connectivity of the inferior frontal gyrus triangular and opercular parts is asymmetrical for the right and the left hemispheres. These findings have implications for understanding the neural bases of human emotion and decision-making, and for their disorders including depression.

* *Corresponding author*. Institute of Science and Technology for Brain-inspired Intelligence, Fudan University, Shanghai, 200433, PR China.
** *Corresponding author*. Institute of Science and Technology for Brain-inspired Intelligence, Fudan University, Shanghai, 200433, PR China.
E-mail addresses: wcheng@fudan.edu.cn (W. Cheng), jianfeng64@gmail.com (J. Feng).
[1] Co-first author.

https://doi.org/10.1016/j.cortex.2019.10.012
0010-9452/

1. Introduction

It has been traditional, for historical reasons based on what was technically possible with the light microscope, to divide the cerebral cortex into different areas based on cytoarchitecture and myeloarchitecture (Brodmann, 1909a; Brodmann, 1909b; Henssen et al., 2016; Öngür, Ferry, & Price, 2003; Ongür & Price, 2000; Vogt, 2009; y Cajal, 1995). For example, the primary visual cortex can be identified by its prominent layer 4, with many granule cells involved in processing the massive visual sensory input from the lateral geniculate nucleus. In another example, motor cortex can be identified by its large pyramidal cells in layer 5, involved in sending motor outputs directly to the spinal cord for fine control of the distal extremities such as the fingers. However, an important way in which to define a cortical area is in terms of the functions it performs, which are related to the inputs that it receives and the regions to which it connects (Rolls, 2016a). The implication is that a different way to divide the cortex into different areas is in terms of the connectivity of each brain area with other brain areas.

In this paper we utilize a method to delineate cortical areas based on their functional connectivity with other brain areas, based on the computational concept that the functional subdivisions of the cortex are likely to be related to where they receive connections from, and where they project to (Rolls, 2016a). In essence, the concept is that the cerebral cortex, and the human brain, can be understood in term of the computations that each brain area performs, based on the inputs that it receives, and where it sends it outputs to (Rolls, 2016a). To achieve this delineation of cortical areas based in their connections with other cortical areas, we measure the functional connectivity of individual voxels in the orbitofrontal cortex and closely related areas the anterior cingulate cortex and inferior frontal gyrus with many different regions of the brain. On the basis of the functional connectivity of each voxel we divide the voxels into different groups or clusters to identify connectional subdivisions of voxels within the area being investigated. Functional connectivity refers to correlations between the fMRI BOLD signal in different brain regions, and reflects direct connections between cortical areas as shown by combined anatomical pathways tracing and functional connectivity analyses in macaques, and also some trans-synaptic effects (Van Essen et al., 2019). An advantage of functional connectivity is that it can reveal trans-synaptic effects, and is non-invasive and can be performed in humans.

In the present case, the voxels of interest are in the orbitofrontal cortex (OFC), the anterior cingulate cortex (ACC), and the inferior frontal gyrus (IFG), because all of these areas are implicated in different ways in emotion, and in emotional disorders including depression (Cheng et al., 2016; Cheng, Rolls, Qiu, Xie, Lyu, et al., 2018; Cheng, Rolls, Qiu, Xie, Wei, et al., 2018; Cheng, Rolls, Qiu, Yang, et al., 2018; Cheng, Rolls, Ruan, & Feng, 2018; Rolls, 2014, 2018, 2019a, 2019c, 2019d; Rolls, Cheng, Du, et al., 2019; Rolls, Cheng, Gong, et al., 2019). This investigation thus goes beyond a previous parcellation of the orbitofrontal cortex (Kahnt, Chang, Park, Heinzle, & Haynes, 2012) not only in terms of the robustness of the analysis (they utilized results from 13 participants, we utilize results from 654 participants for robustness and generalizability), but also because there is a whole set of connected systems involving the OFC, ACC and IFG that are important in emotion and its disorders, so that it is very important to know how all the subparts of these regions are connected. The current investigation is the first to conduct a parcellation of ACC and IFG together with OFC, in order to show how the subparts of these regions are functionally connected, given the importance of at least parts of these regions for emotion, decision-making, and their disorders. Moreover, in the approach described here, the relations and divisions between areas are based on quantitative measures of correlations between the connectivity of areas (identified with the quantitative approach of cluster analysis) with the rest of the brain, whereas anatomical investigations of subnetworks has been based on a qualitative analysis of network subdivisions (Ongür & Price, 2000; Price, 1999, 2006, 2007).

In the present investigation, the connectivity between each voxel in the areas OFC/ACC/IFG and every AAL3 brain area (Rolls, Huang, Lin, Feng, & Joliot, 2019) was measured by the Pearson correlation between their BOLD signals using resting state functional magnetic resonance imaging (fMRI). The concept here is that in a system in which a task is not being performed, the noise-produced perturbations in the system will influence other nodes in the system according to the strength of the connections between any two nodes in the system. The noise in the system is produced by the almost random (Poisson) times of firing of the neurons in the system for a given mean firing rate (Cabral, Kringelbach, & Deco, 2014; Deco, Rolls, Albantakis, & Romo, 2013; Rolls & Deco, 2010), which in turn can be related to factors such as noise in ion channels (Faisal, Selen, & Wolpert, 2008; Rolls & Deco, 2010). A list of abbreviations of AAL3 areas is provided in Table S1 (see Table 1).

2. Methods

2.1. Participants

There were 254 healthy participants subjects (age: 39.7 ± 15.8, Male/Female: 166/88) from Xinan (First Affiliated Hospital of Chongqing Medical School in Chongqing, China); and there were 400 healthy participants (age: 40.6 ± 21.4, Male/Female: 147/253) from the NKI cohort Nathan Kline Institute–Rockland Sample (NKI-RS) dataset (Nooner et al., 2012). All the functional connectivity-driven parcellations were based on the resting-state fMRI data of the 254 subjects in the Xinan cohort and 400 subjects in NKI cohort to provide a sample of 654 subjects for this parcellation analysis. Exclusion criteria for both groups were as follows: current psychiatric disorders and neurological disorders; substance abuse; and stroke or serious encephalopathy. Of note, all of the subjects did not meet DSM-IV criteria for any psychiatric disorders and did not use any drugs that could affect brain function. The collection of the data used in this study was approved by the Research Ethics Committee of the Brain Imaging Center of Southwest University and First Affiliated Hospital of Chongqing Medical School; and as described elsewhere for the NKI data (Nooner et al., 2012). Informed written consent was obtained from each subject.

Table 1 – Abbreviations. A full list of the automated anatomical labelling atlas 3 areas and their abbreviations is provided in Tables S1 and S2. Those used commonly in the main text are shown next for convenience, together with other abbreviations used.

AAL2	automated anatomical labelling atlas 2 (Rolls, Joliot, & Tzourio-Mazoyer, 2015)
AAL3	automated anatomical labelling atlas 3 (Rolls, Huang, et al., 2019)
FC	functional connectivity
MDS	multidimensional scaling
ACCpre	Anterior cingulate cortex, pregenual
ACCsub	Anterior cingulate cortex, subcallosal/ subgenual
ACCsup	Anterior cingulate cortex, supracallosal
ANG	Angular gyrus
HIP	Hippocampus
IFGoperc	Inferior frontal gyrus, opercular part (BA44)
IFGorb	Inferior frontal gyrus, pars orbitalis (part of BA12)
IFGtri	Inferior frontal gyrus, triangular part (BA45)
IPG	Inferior parietal gyrus, excluding supramarginal and angular gyri
ITG	Inferior temporal gyrus
MCC	Middle cingulate & paracingulate gyri
MFG	Middle frontal gyrus
MTG	Middle temporal gyrus
OFCant	Anterior orbital gyrus
OFClat	Lateral orbital gyrus
OFCmed	Medial orbital gyrus
OFCpost	Posterior orbital gyrus
OLF	Olfactory cortex (including part of the olfactory tubercle)
PCC	Posterior cingulate cortex
PHG	Parahippocampal gyrus
Rectus	Gyrus rectus (BA 14)
SFG	Superior frontal gyrus, dorsolateral
SFGmedial	Superior frontal gyrus, medial
SMA	Supplementary motor area
SMG	Supramarginal gyrus
STG	Superior temporal gyrus
VMPFC	Superior frontal gyrus, medial orbital which is often termed the VentroMedial Prefrontal Cortex

2.2. *Image acquisition and preprocessing*

For the Xinan dataset, all the brain images were acquired on a 3.0-T Siemens Trio MRI scanner using a 16-channel whole-brain coil (Siemens Medical, Erlangen, Germany). High-resolution T1-weighted 3D images were acquired using a magnetization-prepared rapid gradient echo (MPRAGE) sequence (echo time (TE) = 2.52 ms; repetition time (TR) = 1900 ms; inversion time (TI) = 900 ms; flip angle = 9°; slices = 176; thickness = 1.0 mm; resolution matrix = 256 × 256; voxel size = 1 × 1 × 1 mm). For each subject, 242 functional images were acquired with a gradient echo type Echo Planar Imaging (EPI) sequence (echo time (TE) = 30 ms; repetition time (TR) = 2000 ms; flip angle = 90°; slices = 32; slice thickness = 3.0 mm; slice gap = 1 mm; resolution matrix = 64 × 64; voxel size 3.4 × 3.4 × 3 mm). During image acquisition, participants were instructed to keep their eyes closed while keeping their head as still as possible without falling asleep. All participants stayed awake during the MRI imaging as confirmed by the participants after the session.

For the NKI dataset, the resting-state fMRI data used in this study were collected from the publicly available Nathan Kline Institute (NKI)/Rockland sample of the 1000 Functional Connectomes project (fcon_1000.projects.nitrc.org/index/enhanced). Scans were collected using a multiband EPI sequence with the following parameters: repetition time (TR)/ echo time (TE) = 650/30 ms, voxel size = 3.0 × 3.0 × 3.0 mm, and 40 slices, covering the whole brain. Individuals' images were viewed one by one to ensure that the whole brain was covered.

Data preprocessing was performed using DPARSF (Chao-Gan & Yu-Feng, 2010) (http://restfMRI.net), which is a toolbox developed for the SPM8 software package. The first 10 echoplanar imaging (EPI) scans were discarded to suppress equilibration effects. The remaining scans of each subject underwent slice timing correction by sinc interpolating volume slices, motion correction for volume to volume displacement, spatial normalization to standard Montreal Neurological Institute (MNI) space using affine transformation and non-linear deformation with a voxel size of 3 × 3 × 3 mm followed by spatial smoothing (8 mm full-width at half-maximum). To remove the sources of spurious correlations, present in resting state blood oxygen level-dependent data, all functional MRI time series underwent band-pass temporal filtering .01–.1 Hz, nuisance signal removal from the ventricles, and deep white matter, and regressing out any effects of head motion using the 24 head motion parameters procedure (Friston, Williams, Howard, Frackowiak, & Turner, 1996). Finally, we implemented additional careful volume censoring ('scrubbing') movement correction (Power et al., 2014) to ensure that head motion artefacts do not drive observed effects. The mean framewise displacement was computed with a framewise displacement threshold of .3 mm, and any participants with a value greater than this were excluded. Global signals were not regressed out for reasons described elsewhere (Cheng et al., 2016). For the NKI dataset, the preprocessing used a similar pipeline.

2.3. *Definition of region of interest*

We selected the orbitofrontal cortex (OFC), inferior frontal gyrus (IFG) and anterior cingulate cortex (ACC) as regions of interest (ROI) using the automated anatomical labelling atlas AAL3 (Rolls, Huang, et al., 2019): Inferior frontal gyrus, opercular part; Inferior frontal gyrus, triangular part; Inferior frontal gyrus pars orbitalis; Superior frontal gyrus, medial orbital; Gyrus rectus; Medial orbital gyrus; Anterior orbital gyrus; Posterior orbital gyrus; Lateral orbital gyrus; Anterior cingulate & paracingulate gyri (which in AAL3 is divided into subgenual, pregenual, and supragenual parts).

2.4. *Connectivity-based parcellation*

The aim of this study was to parcellate the entire OFC/IFG/ACC into distinct subregions based on their resting-state functional connectivities with the whole brain. Specifically, we

first calculated the Pearson correlation coefficient between the time series in each ROI voxel and all the time series from AAL3 regions (137 brain regions) for each subject. This procedure was repeated for all OFC/IFG/ACC voxels (5515 in total) to obtain a 5515 × 137 functional connectivity matrix in which each element i, j of the vector represents the correlation between the i'th voxel of the OFC/IFG/ACC with the j'th AAL3 region. Because all the voxels are in MNI space, the functional connectivity of every voxel in the OFC/IFG/ACC with every brain region in the AAL3 atlas could be measured, and the functional connectivity of each voxel with every AAL3 area could be determined based on the average of the functional connectivity across all 654 participants.

Parcellation was performed using a standard k-means clustering algorithm. This method in combination with this distance measure allowed us to compute parcellations with 24 clusters of voxels in which each cluster had a similar pattern of connectivity with the rest of the brain. The number of clusters for this k-means clustering was determined by statistical tests to check that each cluster had significantly different functional connectivity across the 654 participants with at least one AAL3 area. (The details were as follows. We formed a matrix of the 24 parcels × 137 AAL3 areas of the type shown in Fig. 2, but for each of the 654 participants. Then *t*-tests were performed, with Bonferroni correction for multiple comparisons, to test whether for each of the 24 parcels, at least one of the connectivities with an AAL3 region was significantly different from all other clusters. The large number, 654, of participants in this study contributed to the statistical power of this type of analysis, which has not been possible in any previous investigation.) Factors in the choice of 24 clusters in addition to spatial continuity of voxels in a cluster and statistically significantly different functional connectivity of each cluster with other brain areas, were that with this number of parcels the symmetry index for the orbitofrontal cortex was maximal, and that with k larger than 24 some of the parcels had fewer voxels than 50, with the typical values shown in Fig. 2. An additional criterion was a reduction in the stability of the clustering as k was increased, using the "variation of information" measure (Kahnt et al., 2012). We randomly assigned subjects to two subgroups (N = 327 for each group), averaged the functional connectivity matrix within each subgroup, and computed the clustering for each group for k close to 24 (k = 22–26). Across the 500 randomly selected split-half groups, the similarity (i.e., stability) decreased (increasing "variation of information") as a function of k. Accordingly, the k = 24 cluster solution is optimal in the sense that k = 25 has an increase in the "variation of information".

The cluster analysis/parcellation was performed for all voxels in both the left and right hemispheres simultaneously. This enabled regions with similar connectivity in the two hemispheres to be in the same cluster if they had similar functional connectivity; but also allowed regions with different functional connectivity in the two hemispheres to be in different parcels. To quantify the symmetry of the cluster solutions between the two hemispheres, we computed a similarity index SI_k (Kahnt et al., 2012). This index reflects the percentage overlap between clusters in both hemispheres if one hemisphere is mirrored at the midline. SI_k is computed according to

$$SI_k = \frac{1}{n}\sum_{v=1}^{n}\begin{cases} 1 & \text{if } x_v = x'_v \\ 0 & \text{otherwise} \end{cases}$$

where n is the number of voxels in one hemisphere, and x and x' are the cluster labels of voxel v in the original and mirrored cluster solution, respectively. Because this measure requires that an ROI (e.g., the OFC) is mirror symmetric (i.e., that each voxel exists in both hemispheres), we only included voxels that are present on both sides and discarded voxels that are present on one side only. A high value indicates that the parcels included in the ROI are similar between the left and right hemispheres, where similarity reflects whether voxels are placed in the same cluster.

The robustness of the parcellation was confirmed by measuring the similarity of the parcellations when the parcellation was repeated a number of times with k close to 24; and the optimal number of clusters was measured by checking that each parcel was composed of spatially contiguous voxels, that none of the parcels contained fewer than 50 voxels, by using the symmetry index as described above, and by using the "variation of information" measure as described above.

3. Results

The parcellation based on the resting state fMRI of 654 participants from the NKI and Xinan datasets is shown in Fig. 1, with the average functional connectivity (FC) of the voxels of each of the 24 parcels to the AAL3 brain areas shown in Fig. 2. The parcels and their connectivity are as follows. Each of the parcels had connectivity with at least one of the AAL3 areas shown in Fig. 2 that was significantly different at $p = 1.1 \times 10^{-46}$ (Bonferroni corrected). Fig. 3 illustrates the connections of each parcel on surface maps of the brain. Figs. 1–3 are relevant to the next four sections on parcels in each of the orbitofrontal cortex, anterior cingulate cortex, and left and right inferior frontal gyrus. The exact locations of each parcel in MNI space are shown in Fig. S1 in coronal slices.

3.1. *Orbitofrontal cortex*

The orbitofrontal cortex is implicated in reward value representations, in learning and rapidly changing associations between stimuli and reward vs nonreward, and thereby in emotion (Rolls, 2014, 2018, 2019c, 2019d; Rolls, Cheng, & Feng, 2019). The medial orbitofrontal cortex, areas 13 and 11, is especially implicated in reward valuation, and the lateral orbitofrontal cortex in changing associations between stimuli and reward vs non-reward (Rolls, 2014, 2018, 2019c, 2019d; Rolls, Cheng, & Feng, 2019).

The parcels in the left and right orbitofrontal (Fig. 1) are approximately symmetric, and indeed the voxels on the right and left were in the same cluster (or parcel) for the right and the left. Indeed, the symmetry index for the 6 orbitofrontal cortex parcels was .85 (see below).

The group of medial/mid orbitofrontal cortex areas (parcel 2 medial orbitofrontal cortex), posterior orbitofrontal cortex

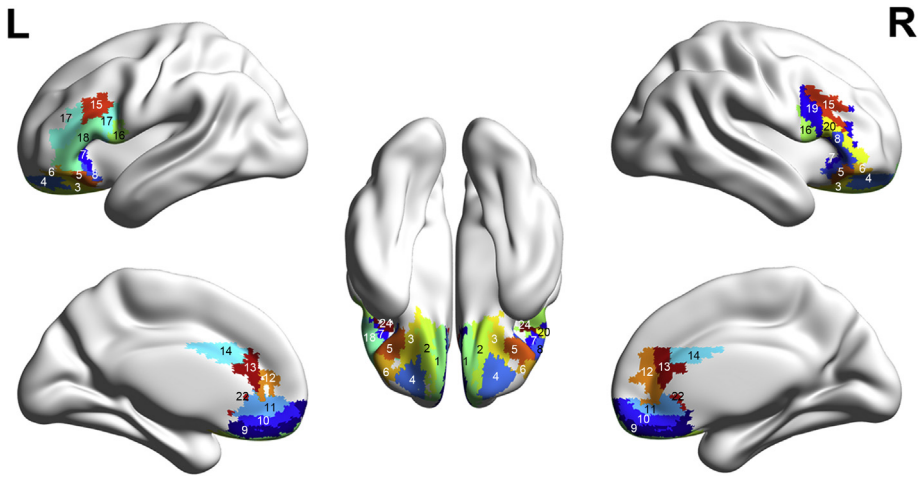

Fig. 1 – Subdivisions or parcels of the OFC/ACC/IFG based on the functional connectivity of individual voxels in the regions with each of the automated anatomical labelling atlas (AAL3 (Rolls, Huang, et al., 2019)) areas of the brain. The 24 subdivisions found are indicated by numbers. The exact locations of each parcel in MNI space are shown in Fig. S1 in coronal slices.

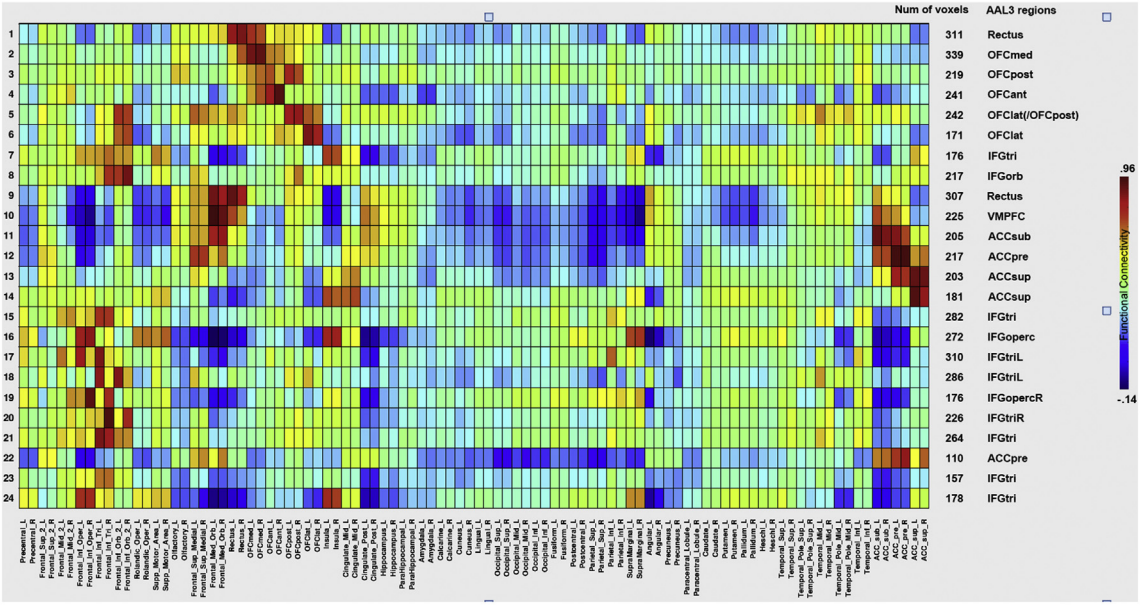

Fig. 2 – Functional connectivity of each of the functional connectivity delineated subdivisions of the OFC/ACC/IFG shown in Fig. 1 (rows) with each of the automated anatomical labelling atlas (AAL3 (Rolls, Huang, et al., 2019)) areas of the brain (columns). High functional connectivity values are shown in brown through red though yellow to low functional connectivity values shown in green to blue. The columns on the right show the number of voxels in each cluster; and the abbreviated name of the AAL3 region that corresponds most closely with each cluster, in order to facilitate understanding of where each cluster is located. Parcels that are present on only the left (L) or right (R) have this as the last letter of the abbreviated name.

(parcel 3), and anterior orbitofrontal cortex (parcel 4) are strongly connected with each other (see Fig. 6), and with temporal cortical areas (Figs. 2 and 3A).

The medial orbitofrontal cortex (parcel 2) has high FC with the anterior and posterior OFC, with the OLF area, and with the gyrus rectus, and its connectivity with the lateral OFC (AAL3 areas OFClat and IFGorb) is smaller (Figs. 2 and 3A). It also has moderate FC with the inferior temporal visual cortex, and with the nucleus accumbens.

The posterior orbitofrontal cortex (parcel 3) has high FC with the anterior and medial OFC, and with the gyrus rectus, and it has some connectivity with the lateral OFC (OFClat and IFGorb2) and inferior frontal gyrus pars triangularis (Figs. 2 and 3A). It also has moderate FC with the parahippocampal gyrus, hippocampus, the posterior mid- and inferior-temporal cortex and fusiform gyrus, the insula, and the mid-cingulate cortex. Parcel 3 (posterior OFC) is thus notable in having moderate FC with a large number of other brain areas, and is

in the graph theory sense a hub. Parcels 2 and 3 have high FC with the OLF region, which is a region at the posterior border of the OFC where it adjoins the olfactory cortex/tubercle.

The anterior orbitofrontal cortex (parcel 4) has high FC with the posterior and medial OFC, and its connectivity with the lateral OFC (OFClat and IFGorb2) is relatively low. It also has high FC with inferior parietal cortex, and anterior inferior temporal cortex, and the middle frontal gyrus (MFG) (Figs. 2 and 3A). It has notably low connectivity with the posterior cingulate cortex, parahippocampal gyrus and hippocampus.

The gyrus rectus (parcel 1) has high FC with the anterior, medial and posterior OFC (parcels 2–4), and OLF, and its connectivity with the lateral OFC (OFClat and IFGorb2) is also considerable (Figs. 2 and 3A). It also has high FC with the angular gyrus, middle temporal gyrus, with other prefrontal cortical areas including FrontalMedorb (or VMPFC), and with the ACCpre and ACCsub and ACCpost but not ACCsup. It has low connectivity with the insula.

The posterior part of the lateral orbitofrontal cortex (parcel 5) has very high FC with IFGOrb2, high with the IFGtri but low with IFGoperc, and moderate FC with superior frontal, the ventromedial prefrontal cortex (VMPFC, AAL3 area FrontalMedOrb), gyrus rectus, posterior OFC, OLF, middle and posterior cingulate, hippocampus, parahippocampal gyrus, left angular gyrus, all temporal cortical areas, the ACCpre and ACCsub but not ACCsup (Figs. 2 and 3A). This parcel is larger on the right as shown in coronal slices Fig. 1 (right 128 voxels, left 115), and the AAL3 area OFClat is larger on the right than the left. (Similarly, parcel 8, the connected and related orbital part of the inferior frontal gyrus, is larger on the right than the left (171 vs 46 voxels).) This is consistent with the lateral orbitofrontal cortex and inferior frontal gyrus areas pars orbitalis areas being larger on the right, compared to the left where they may be reduced in size to accommodate the larger inferior frontal gyrus areas that are part of Broca's area on the left.

The anterior part of the lateral orbitofrontal cortex (parcel 6) has very high FC with IFGOrb2, high with the IFGtri but low with IFGoperc, gyrus rectus, very high with lateral OFC, left angular gyrus, and mid and inferior temporal gyri. Parcel 6 has overlap with AAL3 area OFClat (Figs. 2 and 3A).

The lateral orbitofrontal cortex areas, and the gyrus rectus, are notable in having moderate FC with the angular gyrus.

3.2. *Anterior cingulate cortex and ventromedial prefrontal cortex*

The anterior cingulate cortex receives information from the orbitofrontal cortex, and is implicated in learning associations between actions and reward vs punishment outcomes (Rolls, 2019; Rushworth, Kolling, Sallet, & Mars, 2012).

The anterior cingulate cortex parcel 14 which is supracallosal and posterior has high FC with IFGoper but not IFGtri, and moderate FC with other prefrontal areas, supplementary motor area, insula, midcingulate, supramarginal gyrus, caudate, putamen, globus pallidus, superior temporal, ACCsup (where this parcel is located) (Figs. 2 and 3B).

The anterior cingulate cortex parcel 13 which is supracallosal and less posterior has high FC with superior frontal, IFGoperc but not IFGtri, supplementary motor area, insula, midcingulate, supramarginal gyrus, putamen, pallidum, superior temporal, ACCsup (where this parcel is located). These two supracallosal ACC parcels are notable in having moderate FC with the supramarginal gyrus (Figs. 2 and 3B).

The pregenual anterior cingulate cortex (parcel 12) has high FC with FrontalSupMed, FrontalMedOrb, Superior Frontal Gyrus, OFCpost, midcingulate, post cingulate, left angular, and ACCpre (where this parcel is located), ACCsub, and ACCsup (Figs. 2 and 3B).

The ventromedial prefrontal cortex (upper part, parcel 11, which includes the subcallosal anterior cingulate cortex) has high FC with ACCsub (where this parcel is located), with ACCpre which is higher than ACCsup, superior frontal, OLF, FrontalSupMed, FrontalMedOrb or VMPFC (especially high), rectus, posterior cingulate with some mid-cingulate, nucleus accumbens, hippocampus, left angular gyrus (Figs. 2 and 3B).

The ventromedial prefrontal cortex (middle part, parcel 10) has high FC with superior frontal, OLF, SFGmedial, FrontalMedOrb (i.e., VMPFC where this parcel is located), rectus, OFCpost, posterior cingulate, hippocampus and parahippocampal cortex, angular bilaterally, precuneus, middle temporal, temporal pole, ACCsub and ACCpre but not ACCsup (Figs. 2 and 3B).

The ventromedial prefrontal cortex (lower part, parcel 9, which includes part of the gyrus rectus) has very similar FC to parcel 10 except for lower FC with ACCsub and ACCpre, but higher FC with angular, and rectus (Figs. 2 and 3B). This fits with parcels 10 and 9 being important areas in reward and memory with links to language.

Parcels 9–12 in the ACCpre and VMPFC are notable in having moderate FC with the angular gyrus and with anterior parts of the temporal lobe (Fig. 3B).

3.3. *Left lateral inferior frontal gyrus*

The left inferior frontal gyrus is part of Broca's area and is implicated in language production (Amunts & Zilles, 2012).

In the inferior frontal gyrus, pars triangularis, Parcel 15 (which is bilateral, and at the top of the IFG) has high FC with Middle Frontal Gyrus, IFGtri (where this parcel is located), IFGorb (bilaterally, part of the lateral orbitofrontal cortex), left fusiform, inferior parietal, posterior temporal areas, with the supramarginal and angular cortex, and with the caudate and putamen (Figs. 2 and 3D).

In the inferior frontal gyrus, pars triangularis (area 45), Parcel 18 (on the left only) has high FC with superior and middle frontal gyrus, IFGtri (where the parcels is located), IFGorb (especially high on the left) and lateral orbitofrontal cortex; angular, part of the supramarginal, and inferior parietal cortices; supplementary motor area; the medial superior frontal gyrus (FrontalSupMed); the posterior orbitofrontal cortex; gyrus rectus; and many temporal lobe cortical areas including especially anteriorly and the middle temporal gyrus (Figs. 2 and 3D).

In the inferior frontal gyrus, pars triangularis and opercularis, Parcel 17 (on the left only) has high FC with precentral, middle Frontal Gyrus, IFGtri and IFGoperc, IFGorb (especially left), supplementary motor area, OFCant (on the left), left insula, left fusiform, supramarginal gyrus, and posterior inferior temporal (Figs. 2 and 3D).

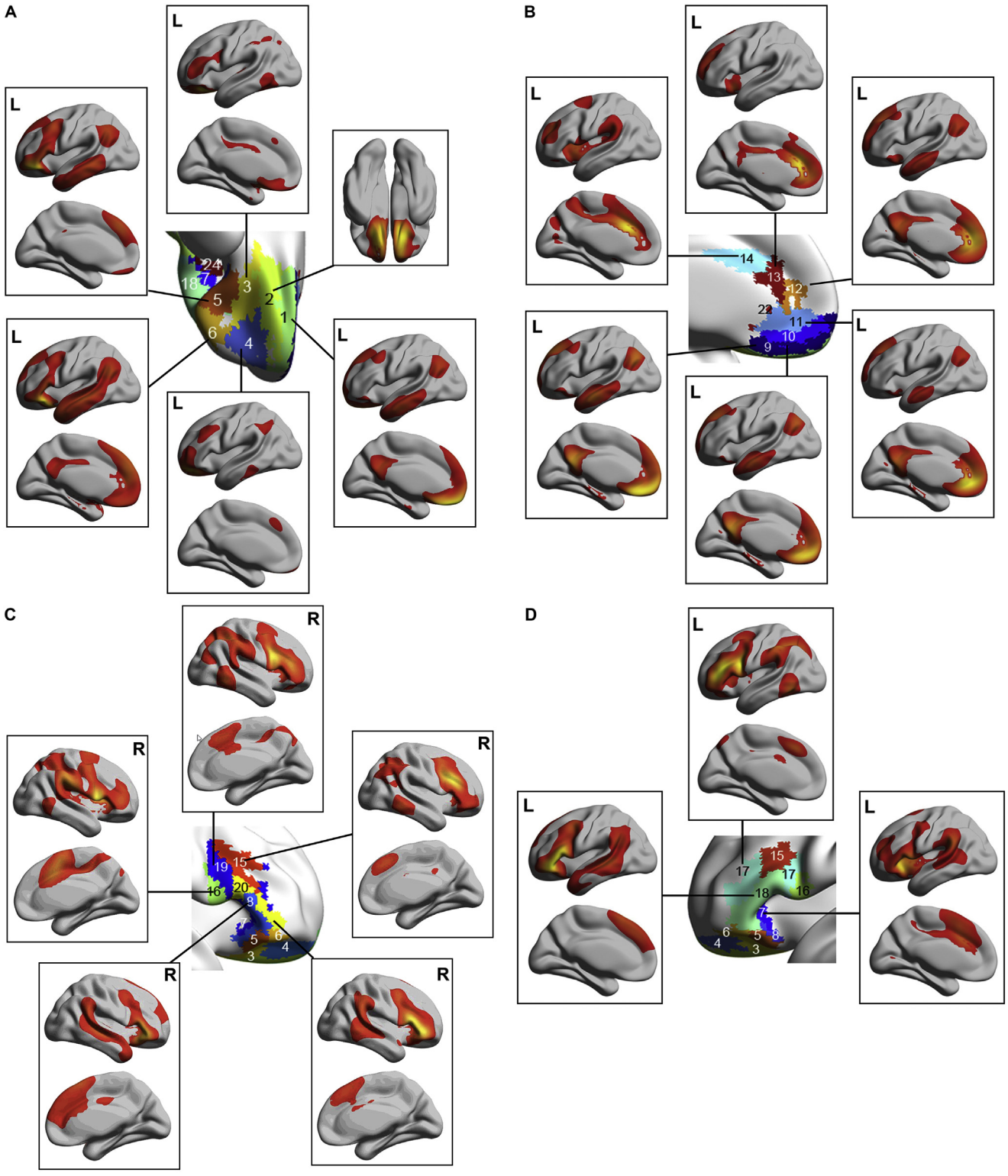

Fig. 3 – A. Surface maps showing the connectivity of each parcel. A. For the orbitofrontal cortex. B. For the anterior cingulate cortex. C. For the inferior frontal gyrus right and symmetric parcels. D. For the inferior frontal gyrus left asymmetric parcels. The functional connectivities have been thresholded at 0.3.

In the inferior frontal gyrus, pars opercularis, Parcel 16 has high FC with precentral and postcentral, IFGoperc (of which it is a part), Rolandic operculum, Supplementary Motor area, insula bilaterally (very high), mid-cingulate, supramarginal (high FC bilaterally), putamen, pallidum (Figs. 2 and 3D).

In the inferior frontal gyrus, pars orbitalis parcel 7 (which is bilateral) has high FC with IFGorb (where it is located), the supracallosal part of the anterior cingulate cortex and the mid-cingulate cortex, IFGtri and IFGoperc, supplementary motor area, insula, cingulate mid, Supramarginal left and right (but not angular gyrus), putamen, pallidum, and superior temporal (Figs. 2 and 3D).

In the inferior frontal gyrus, pars orbitalis parcel 8 (which is bilateral) has high FC with IFGorb (where it is located); notably with the lateral orbitofrontal cortex (OFClat), anterior cingulate cortex supracallosal part, and the mid cingulate cortex; IFGtri; OFCpost; supplementary motor area; insula; supramarginal gyrus bilaterally, mid- and superior temporal areas, and superior medial frontal cortex (Figs. 2 and 3D).

3.4. *Right lateral inferior frontal gyrus*

The right inferior frontal gyrus is implicated in some types of behavioral inhibition including some types of impulsivity (Aron, Robbins, & Poldrack, 2014; Deng et al., 2017). The right inferior frontal gyrus may especially convey information from non-reward systems in the lateral orbitofrontal cortex and orbital part of the inferior frontal gyrus to premotor areas (Rolls, 2019c; Rolls, Cheng, Du, et al., 2019; Rolls, Cheng, & Feng, 2019).

IFGtri (posteriorly) Parcel 19 has high FC with precentral gyrus, IFGoperc (right especially high), Middle Frontal Gyrus (right), IFGtri (right, where this parcel is located), supplementary motor area (especially right), insula, fusiform, superior and inferior parietal, supramarginal (especially on right), and posterior temporal (Figs. 2 and 3C).

IFGtri (and IFGorb) Parcel 20 has high FC with IFGtri and IFGorb (where it is located), Middle FG, IFG opercular (area 44, right), OFCpost (right), supramarginal (right), posterior superior and middle temporal (right), with the inferior parietal cortex, and with the right supramarginal cortex (Figs. 2 and 3C).

3.5. *Graphical representation of the connectivity*

The result of multidimensional scaling (MDS) on the correlation matrix of Fig. 2 is shown in Fig. 4. The distance in this space reflects how different the connectivity is of each parcel. This diagram is complemented by Fig. 5 which shows by the thickness and colour of the lines the strength of the functional connectivity between the different parcels, shown in this case on a view of the brain. It is also complemented by Fig. 6 which shows the functional connectivities between the parcels as a matrix. The description that follows refers to the MDS space in Fig. 4, but reference to Figs. 5 and 6 will also be useful.

The OFC areas OFCmedial, OFCposterior, and OFCanterior are close together. Interestingly, the IFG triangular superior parcel (15) is close to these OFC areas.

The lateral OFC areas (6 and 5) are somewhat separated from these medial OFC areas, and interestingly the gyrus

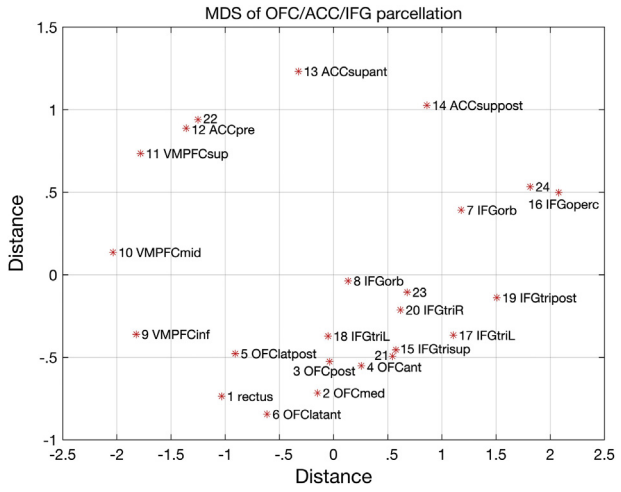

Fig. 4 – Multidimensional scaling for the connectivity matrix shown in Fig. 2. The parcels are named after the AAL3 name of the region that best describes the location of each parcel, but it must be noted that each parcel based on the functional connectivity does NOT correspond exactly to an AAL3 area. Abbreviations: OFC - orbitofrontal cortex; ACC - anterior cingulate cortex; IFG - inferior frontal gyrus. Names: 1 gyrus rectus; 2 OFC medial; 3 OFC posterior; 4 OFC anterior; 5 OFC lateral posterior; 6 OFC lateral anterior; 7 IFG orbital; 8 IFG orbital; VMPFC inferior; 10 VMPFC middle; 11 VMPFC superior; 12 ACC pregenual; 13 ACC supracallosal anterior; 14 ACC supracallosal posterior; 15 IFG triangular superior; 16 IFG opercular; 17 IFG triangular Left; 18 IFG triangular Left; 19 IFG triangular posterior; 20 IFG triangular Right.

rectus (1) is close to these lateral OFC areas. The IFG orbital parcel 8 is not very close to parcels 5 and 6, and IFG orbital parcel 7 is closer to the other IFG areas.

The VMPFC parcels 9, 10 and 11 are well separated from other parcels, with VMPFC inferior (9) closest to OFC areas, and VMPFC superior (11) closest to ACC pregenual (12). The subgenual/subcallosal cingulate cortex will be within parcel 11.

The three ACC parcels are well spread out from other nodes, and from each other. It is notable that the ACC supracallosal anterior parcel is not close to the OFC lateral parcels, even though both represent punishers and non-reward (Rolls, 2019c, 2019d). This is probably because the ACC supracallosal areas have connectivity with movement-related areas.

The IFG parcels are in a region of the right of the MDS space in Fig. 4, with, interestingly, parcel 17 IFG triangular superior L and parcel 18 IFG triangular superior R relatively close to the medial OFC areas in parcels 2, 3 and 4.

3.6. *Correlations between the connectivity of the parcels*

The correlations between the 24 different parcels defined by their functional connectivity with all areas in the AAL3 atlas (Rolls, Huang, et al., 2019) are shown in Fig. 6. First, it should be made clear that all the parcels are statistically different, in that the least significant p value for the difference of a functional connectivity of any two parcels with an AAL3 brain area

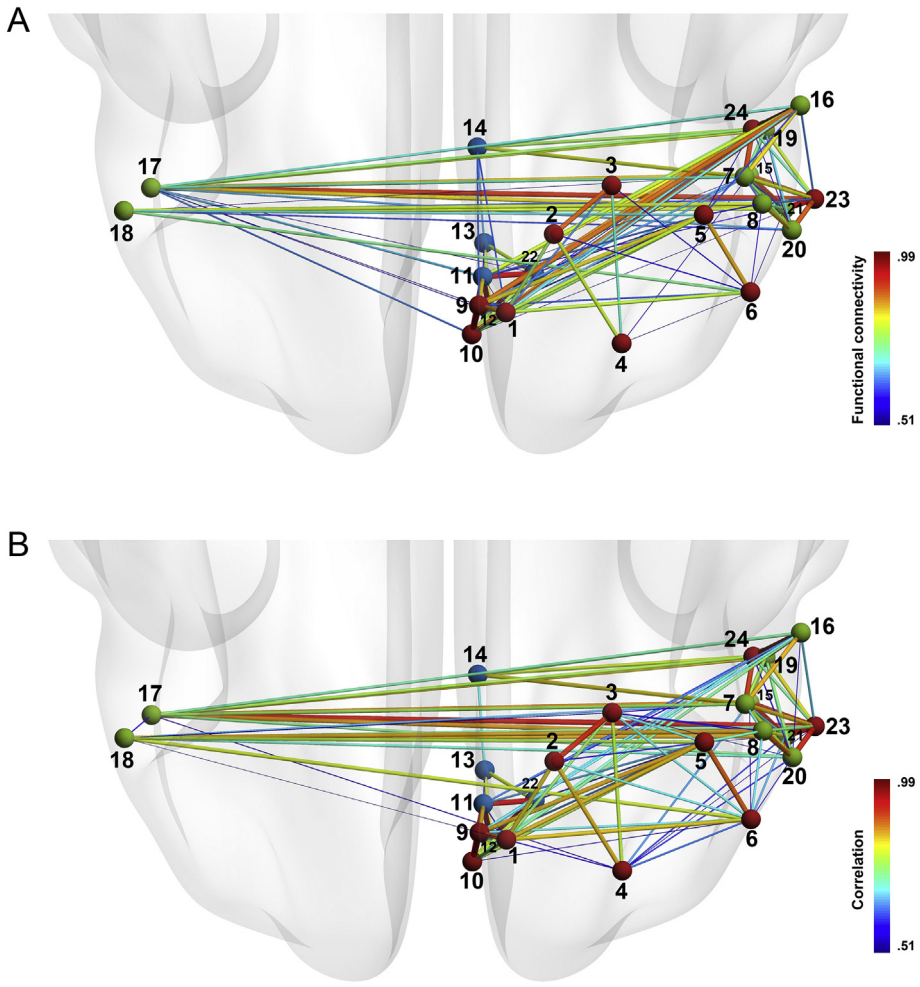

Fig. 5 – A. Similarity of different parcels in the orbitofrontal cortex, anterior cingulate cortex, and inferior frontal gyrus based on the functional connectivity (FC) of each parcel with the other parcels that is illustrated in Fig. 6. The color of the edges and their thickness represents the strength of the functional connectivity. The color of the parcel nodes indicates the brain region: orbitofrontal cortex - red; anterior cingulate and ventromedial prefrontal cortex - green; inferior frontal gyrus-yellow. The two parcels that are asymmetric in the left inferior frontal gyrus are placed on the left of the brain (looking down on a view of the orbitofrontal cortex). B. The similarity (Correlation) based on the functional connectivity of each parcel with the whole brain (i.e., all AAL3 areas).

is $p = 10^{-134}$. Fig. 6 shows that Parcels 1–7 are correlated with each other. These are the orbitofrontal cortex parcels. Parcels 9–13 are correlated with each other, as are the VMPFC and ACC parcels, with the exception of the most posterior supracallosal ACC parcel. The correlation matrix shows that parcel 22, a small parcel at the junction of VMPFC and ACC, should be included with this group. Parcels 15–24 (except for 22) form a third group, all involving inferior frontal gyrus areas. Fig. 6 shows that parcel 7 in the IFG orbital part correlates with this IFG group, whereas parcel 8 also in the IFG orbital part correlates only partly with the IFG group, and partly with the OFC group.

For comparison with what is shown in Fig. 6, we also directly measured the functional connectivity between the 24 parcels by using the correlation between the BOLD signals for every pair of parcels. The BOLD signal for each parcel was measured by taking the average of the BOLD signal across all voxels within each parcel. The resulting functional correlation matrix was very similar to that shown in Fig. 6, and indeed the correlation between the two correlation matrices was .91. This shows that the functional connectivity measured directly from the BOLD signal correlations between the 24 OFC/ACC/IFG parcels was similar to that measured from the correlations between the BOLD signal in each of the 24 parcels with all AAL3 areas. An almost identical result was obtained when the functional connectivity directly measured using the BOLD signal from the 24 parcels was compared to that measured from the correlations between the BOLD signal in each of the 24 parcels with all AAL3 areas except AAL3 areas in the OFC/ACC/IFG. These results are consistent with the functional connectivities measured between the 24 parcels in the orbitofrontal cortex/anterior cingulate cortex/inferior frontal gyrus reflecting both connectivity between the 24 parcels, and the connectivity of each of the parcels with other brain areas.

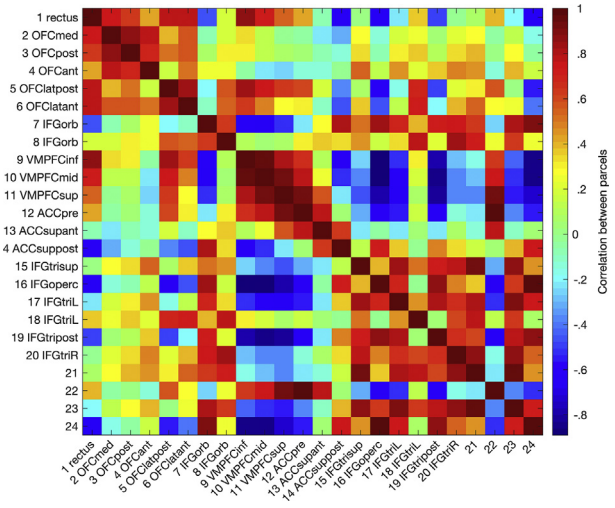

Fig. 6 – Correlations between the different parcels defined by their functional connectivity with all areas in the AAL3 atlas (Rolls, Huang, et al., 2019).

3.7. *Symmetry of the parcellation in the two hemispheres*

The similarity index for the parcels within the orbitofrontal cortex (OFC) ROI was .85, for the anterior cingulate cortex (ACC) was .94, and for the inferior frontal gyrus (IFG) was .27. This quantifies what is evident in Figs. 1 and 2, that for the OFC and ACC, voxels in the left and right hemispheres have similar functional connectivity with other brain areas, and therefore are clustered together by k-means into the same parcel. In contrast, for the IFG, several of the parcels on the Left and Right do not have similar connectivity, so the voxels in the left and right IFG are placed into different parcels.

4. Discussion

4.1. *The connectivity and some of the implications*

The findings of this parcellation of the orbitofrontal cortex, anterior cingulate cortex, and inferior frontal gyrus based on the functional connectivity with the whole brain include the following.

First, three parcels (2–4) located mainly in areas 13 and 11 in the medial/mid orbitofrontal cortex had strong connectivity with each other, and moderate connectivity with posterior to mid-temporal cortical areas and insula (which are likely to provide visual, auditory and taste inputs), with the cingulate cortex (which are likely to provide outputs to action-outcome systems), and with the parahippocampal gyrus and hippocampus (which are related to memory) (Rolls, 2016a, 2019c; 2019d). Many rewards are represented in this region (Grabenhorst & Rolls, 2011; Rolls, 2019c, 2019d).

Second, two parcels (5 and 6) located mainly in area 12 the lateral orbitofrontal cortex have interesting connectivity with the left angular gyrus which is related to language, as well as with widespread areas of the temporal lobe cortex; the parahippocampal gyrus and hippocampus; and with the triangular part of the inferior frontal gyrus (which may provide for outputs), as well as with the supracallosal anterior cingulate cortex. Many punishers and non-reward are represented in this region (Grabenhorst & Rolls, 2011; Rolls, 2019c, 2019d). Two parcels in the inferior frontal gyrus, pars orbitalis (8 and 7 especially on the right) have strong connectivity with the lateral orbitofrontal cortex and also with a number of movement related areas (the supplementary motor area, insula, midcingulate and supracallosal anterior cingulate, supramarginal left and right). These inferior frontal gyrus pars orbitalis areas may relate the lateral orbitofrontal cortex to brain areas involved in movement initiation.

Third, parcels in the ventromedial prefrontal cortex parcels (9, 10 and 11) and the pregenual anterior cingulate cortex (parcel 12) have connectivity with the angular gyrus, with anterior parts of the temporal lobe (Fig. 3B); with the orbitofrontal cortex; and with the parahippocampal gyrus and hippocampus, posterior cingulate cortex and precuneus all of which are implicated in memory (Rolls, 2016a; 2019c, 2019d). This fits with these areas being important in reward, decision-making, and memory, with interesting links to language (Rolls, 2016a, 2019c, 2019d).

Fourth, in the supracallosal anterior cingulate cortex, parcels 13 and 14 have connectivity with the mid-cingulate cortex, supplementary motor area and basal ganglia; with the inferior frontal gyrus pars opercularis (BA 44) rather than with pars triangularis (BA45); and with the supramarginal gyrus (BA 40) rather than the angular gyrus (BA 39). These supracallosal anterior cingulate areas activated by punishers and non-reward (Rolls, 2016a, 2019c, 2019d) are thus more closely related to the brain areas involved in the initiation of movements, and perhaps to somatosensory function and phonology in which the marginal gyrus is implicated.

Fifth, the left inferior frontal gyrus, pars triangularis (area 45), and pars opercularis (area 44) involved in language as part of Broca's area and with functional connectivity with the angular, supramarginal, and inferior parietal cortices, with anterior (area 45) and posterior (area 44) temporal cortical areas also interestingly had some functional connectivity with the orbitofrontal cortex, and may thereby provide a route for some orbitofrontal cortex areas to link to language systems.

4.2. *Functional connectivity parcellation and cytoarchitecture*

There is some interesting similarity between the subdivisions of the OFC and ACC produced by cytoarchitecture (shown in Fig. 7) (Öngür et al., 2003) and the functional connectivity parcellation (Fig. 1). For example, Parcel 1 may correspond partly to the gyrus rectus, areas 14 and 11 m. Parcel 2 in the medial orbitofrontal cortex may correspond partly to area 13 m. Parcel 3 in the posterior part of the mid (medial) orbitofrontal may correspond partly to area 13 l. Parcel 4 in the anterior part of the mid (medial) orbitofrontal may correspond partly to area 11 l but also part of 10p. Parcel 5 in the posterior lateral OFC may correspond partly to area 12 m. Parcel 6 in the anterior lateral OFC may correspond partly to area 12r. A different cytoarchitectural analysis (Henssen et al., 2016) corresponds less well with the functional parcellation described here.

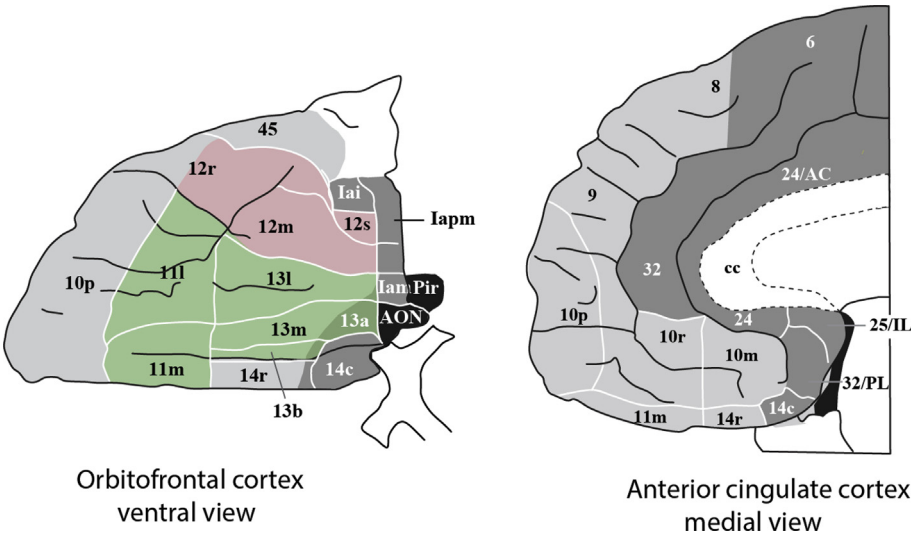

Fig. 7 – Cytoarchitectural divisions of the orbitofrontal cortex (left, areas 13, 11 and 12) and anterior cingulate cortex (right, areas 24, 32 and 25) (modified from (Öngür et al. (2003)). The medial orbitofrontal cortex is in green; the lateral orbitofrontal cortex is in red. Area 14 is in the gyrus rectus. Area 45 is the inferior frontal gyrus, pars orbitalis.

However, more importantly, the functional connectivity parcellation provides information about connectivity, which the cytoarchitecture does not, and the connectivity is considered next using the evidence provided in Figs. 2–6. The following discussion focusses on some of the key differences between the different parcels, using the functional connectivity values in Fig. 2. In Fig. 2, the strongest FCs provide an indication of the AAL3 region(s) where the parcel is located, because there is typically high FC of the voxels within an AAL3 region.

4.3. *Relation to areas implicated in language*

One aspect of interest is with respect to areas implicated in language. The connectivity of the angular gyrus (on the left especially) is high with parcels in the angular gyri (18); and VMPFC/ACC (9, 10, 11, 12), gyrus rectus (1), and lateral orbitofrontal cortex (5 and 6). The connectivity of the supramarginal gyrus (mostly bilaterally) is high with parcels in the inferior frontal gyrus (7, 16, 17, 18, 19, 20), and with the supracallosal anterior cingulate cortex posterior part (14) and ACC pregenual parcel 12. A very interesting finding shown in Fig. 4 is that the inferior frontal gyrus areas (IFG) implicated in language (especially on the left) are quite close to orbitofrontal cortex areas (e.g., the anterior and posterior orbitofrontal cortex) in the multidimensional space, and relatively far from the ventromedial prefrontal cortex (VMPFC) and the anterior cingulate cortex (ACC). This provides interesting evidence for a close relationship between what is represented in the orbitofrontal cortex and language. Consistent with this, cognitive inputs at the language level can bias reward representations of odour, taste and flavour in the orbitofrontal cortex (de Araujo, Rolls, Velazco, Margot, & Cayeux, 2005; Grabenhorst, Rolls, & Bilderbeck, 2008); and the reported subjective pleasantness of many rewarding stimuli, including taste, flavor, and somatosensory stimuli is linearly related to the activations of the medial/mid orbitofrontal cortex (Grabenhorst, D'Souza, Parris, Rolls, & Passingham, 2010; Grabenhorst, Rolls, & Parris, 2008; Grabenhorst, Rolls, Parris, & D'Souza, 2010).

4.4. *Symmetry*

Second, the orbitofrontal parcels are remarkably symmetric across the midline (Similarity Index .85), whereas in line with the lateralization of language and the importance of the inferior frontal gyrus in language (Amunts & Zilles, 2012; Clos, Amunts, Laird, Fox, & Eickhoff, 2013), the inferior frontal gyrus is asymmetric (SI = .27). The symmetry of the orbitofrontal connectivity (and therefore parcellation) is consistent with the findings that there is little evidence for strong lateralization of activations of the orbitofrontal cortex in task-related fMRI, with some differences in individual studies not generally found when large numbers of studies are considered (Grabenhorst & Rolls, 2011). Interestingly, the anterior cingulate cortex has a high SI of .94, reflecting great symmetry in the voxel-level connectivity of the right and left anterior cingulate, an area that receives reward value information from the orbitofrontal cortex, and is then involved in learning actions to obtain the rewards signaled by the orbitofrontal cortex (Rolls, 2019a).

4.5. *Functional regions of the orbitofrontal cortex*

Third, there is much evidence for a hedonic map in the orbitofrontal cortex, with many rewards and subjectively pleasant stimuli represented in the medial orbitofrontal cortex, and many unpleasant stimuli and non-rewards represented in the lateral orbitofrontal cortex (Grabenhorst & Rolls, 2011; Rolls, 2019c). This applies for example to monetary reward and loss (O'Doherty, Kringelbach, Rolls, Hornak, & Andrews, 2001; Xie et al., 2019), olfactory stimuli (Rolls, Kringelbach, & de Araujo, 2003), and not winning in a reversal task indicating that reversal should occur (Kringelbach & Rolls, 2003). Does

the connectivity of the medial/mid orbitofrontal cortex differ from that of the lateral orbitofrontal in any way that may illuminate this? One difference is that the medial orbitofrontal cortex areas tend to have high functional connectivity with the pregenual anterior cingulate cortex in both of which rewards are represented. In contrast, the lateral orbitofrontal cortex including AAL3 areas such as OFClat and the inferior frontal gyrus orbital part has high functional connectivity with the supracallosal anterior cingulate cortex, in both of which unpleasant stimuli and non-reward are represented (Rolls, Cheng, Gong, et al., 2019). From Fig. 2, differences in the FC of the medial OFC (parcels 2, 3, and 4) from the lateral OFC (parcels 5 and 6) are as follows. The lateral OFC has higher FC with the inferior frontal gyrus, SFGmedial, ACCpost, angular gyrus, and mid-temporal cortex. Parcel 6 (lateral OFC, anterior parcel) has low FC with the ACCsub and Pre, but parcel 5 posteriorly does not. Parcels 7 and 8 in the orbital part of the inferior frontal gyrus have high FC with the supracallosal part of the anterior cingulate cortex, IFCopercular, SFGmedial, SMA, caudate, putamen and pallidum, insula, and supramarginal gyrus. Parcels 7 and 8 may thus relate to unpleasantness (because of the association with the supracallosal anterior cingulate cortex), and in line with this, have high FC with the insula, the anteroventral part of which is related to autonomic function and much of it to somatosensory function. Parcels 7 and 8 can thus be considered as a lateral part of the orbitofrontal cortex, connecting with the supracallosal part of the anterior cingulate cortex, both involved in punishers and non-reward, consistent with a more detailed analysis (Rolls, Cheng, Gong, et al., 2019). The medial OFC has high FC with the inferior parietal cortex, and low with the angular gyrus.

The main parcels with high functional connectivity with the insula are in the IFGtri, IFGoperc, IFGorb and ACCsup, with the OFCpost having some connectivity. This may reflect the insula being used as part of a viscero-motor region for outputs to autonomic function (Rolls, 2016b).

The larger extent of the lateral orbitofrontal cortex areas found in parcels 5 and 6 on the right, and the parcels in or near the orbital part of the inferior frontal gyrus on the right (8 and 20, see Fig. S1) are of especial interest, for these areas on the right are implicated in depression, in that voxels in parts of these regions have high functional connectivity in depression with the angular gyrus, temporal cortex, the precuneus, and the posterior cingulate cortex (Cheng et al., 2016; Cheng, Rolls, Qiu, Xie, Wei, et al., 2018; Cheng, Rolls, Qiu, Yang, et al., 2018; Rolls, Cheng, Du, et al., 2019). These findings are consistent with the hypothesis that increased attractor-related activity in the lateral orbitofrontal cortex non-reward system contributes to depression (Rolls, 2016c, 2018; Rolls, Cheng, & Feng, 2019), and that the right inferior frontal gyrus provides a route to premotor systems for behavioral output that relates to depression (Rolls, Cheng, Du, et al., 2019). The right inferior frontal gyrus is further implicated in routes to action, in that this system is activated in the stop-signal task (Deng et al., 2017), and damage to the right inferior frontal gyrus in humans impairs behavioral inhibition in the stop-signal task (and in this sense increases response-related impulsivity) (Aron et al., 2014). If these lateral orbitofrontal and inferior frontal gyrus regions have increased connectivity and are overactive in depression, then behavioural output to action systems may be diminished with too much inhibition of behavior; and if these regions are damaged, behavior may be insufficiently stopped resulting in a type of impulsiveness (Rolls, 2019c; Rolls, Cheng, Du, et al., 2019; Rolls, Cheng, & Feng, 2019).

4.6. *Comparison with connections in the macaque*

Comparison of the functional connectivity between the different parcels shown in Figs. 5B and 6, and the anatomical connections of the orbitofrontal cortex and anterior cingulate in the macaque shown in Fig. 19 of Carmichael and Price (1996), indicates the following. (Carmichael and Price identified medial prefrontal networks, which included the anterior cingulate cortex, and orbital networks.) In humans, parcels 2, 3, and 4 form one network for the medial orbitofrontal cortex. For the lateral orbitofrontal cortex, parcels 5 and 6 are part of a network which includes gyrus rectus and left inferior frontal gyrus pars triangularis (18) and inferior frontal gyrus pars orbitalis (8). Another network includes parcels in the ventromedial prefrontal cortex and the pregenual and subgenual anterior cingulate cortex (9,10,11,12) and posterior lateral orbitofrontal cortex (5). Another network includes the right and bilateral inferior frontal gyrus areas (7, 8, 15, 16, 19, 20, 24), which notably include parcel 8 in IFGorb. Last, the left inferior frontal gyrus (parcels 17 and 18) connect to other IFG regions, OFC lat (5,6) and IFGorb (8). In the macaque Carmichael and Price (1996) investigated the OFC and ACC, and did not include the inferior frontal gyrus, or of course any connectivity with language areas, which was so interesting in the human functional connectivity. In an 'orbital prefrontal' network they showed a number of subregions in the medial orbitofrontal cortex BA areas 13 and 11 with connections with subregions in the lateral orbitofrontal cortex BA area 12. In contrast, in humans the medial and lateral orbitofrontal networks were more separate, and the lateral orbitofrontal cortex continues round the inferior prefrontal convexity to include at least inferior frontal gyrus orbital part especially on the right. Carmichael and Price (1996) identified a macaque 'medial prefrontal network' which included the anterior cingulate cortex, but did not distinguish pregenual from supracallosal parts of the ACC which have quite different functional connectivity in humans, and also showed connectivity with a single VMPFC region (BA 10 m) rather than the several VMPFC subregions identified here in humans.

We further note that the present investigation goes beyond that of Kahnt et al. (2012), by including in the parcellation in addition to the orbitofrontal cortex, for the first time also the anterior cingulate cortex and medial prefrontal cortex, so that we could directly compare the functional connectivity of these nearby regions with other brain areas (Fig. 2), and with each other (Fig. 6), because all are implicated in different ways in emotion and action (Rolls, 2019b, 2019c, 2019d; Rolls, Cheng, & Feng, 2019); and by including 654 participants compared to 13.

In conclusion, the new findings described here include the following. First, in areas BA 13 and 11 in the medial/mid orbitofrontal cortex had strong connectivity with each other, and moderate connectivity with posterior to mid-temporal

cortical areas and insula (which are likely to provide visual, auditory and taste inputs), with the cingulate cortex (which are likely to provide outputs to action-outcome systems), and with the parahippocampal gyrus and hippocampus (which are related to memory). Second, parcels in area BA 12 the lateral orbitofrontal cortex have connectivity with the left angular gyrus, as well as with the temporal lobe cortex; the parahippocampal gyrus and hippocampus; and with the triangular part of the inferior frontal gyrus (which may provide for outputs), as well as with the supracallosal anterior cingulate cortex. Parcels in the inferior frontal gyrus, pars orbitalis have strong connectivity with the lateral orbitofrontal cortex and with movement-related areas, and may provide a route from the lateral orbitofrontal cortex to brain areas involved in movement initiation. Third, parcels in the ventromedial prefrontal cortex and pregenual anterior cingulate cortex have connectivity with the orbitofrontal cortex; angular gyrus; temporal lobe, parahippocampal gyrus and hippocampus, posterior cingulate cortex and precuneus. This fits with these areas being important in reward, decision-making, and memory, with interesting links to language. Fourth, the supracallosal anterior cingulate cortex has connectivity with the orbitofrontal cortex and movement-related areas, so may provide a route to movement from the orbitofrontal cortex. Fifth, the left inferior frontal gyrus involved in language has functional connectivity with the orbitofrontal cortex, and may thereby provide a route for some orbitofrontal cortex areas to link to language systems.

Funding

J.F. is partially supported by the key project of Shanghai Science & Technology Innovation Plan (No. 15JC1400101 and No. 16JC1420402) and the National Natural Science Foundation of China (Grant No. 71661167002 and No. 91630314). The research was also partially supported by the Shanghai AI Platform for Diagnosis and Treatment of Brain Diseases (No. 2016–17). The research was also partially supported by Base for Introducing Talents of Discipline to Universities No. B18015. W.C. is supported by grants from the National Natural Science Foundation of China of China (No.81701773, 11771010), Sponsored by Shanghai Sailing Program (No. 17YF1426200) and the Research Fund for the Doctoral Program of Higher Education of China (No. 2017M610226). W. Cheng is also sponsored by Natural Science Foundation of Shanghai (No. 18ZR1404400). J. Qiu was supported by the National Natural Science Foundation of China (31271087; 31470981; 31571137; 31500885), National Outstanding young people plan, the Program for the Top Young Talents by Chongqing, the Fundamental Research Funds for the Central Universities (SWU1509383), Natural Science Foundation of Chongqing (cstc2015jcyjA10106), General Financial Grant from the China Postdoctoral Science Foundation (2015M572423). P. Xie is supported by National Key R&D Program of China (2017YFA0505700).

The funding agencies took no part in the design or implementation of the research.

No part of the study procedures was pre-registered prior to the research being conducted. We report in this paper how we determined our sample size, all data exclusions, all inclusion/exclusion criteria, whether inclusion/exclusion criteria were established prior to data analysis, all manipulations, and all measures in the study, in the Methods section. The neuroimaging data from NKI is publicly available at http://fcon_1000.projects.nitrc.org/indi/pro/nki.html. The conditions of the ethics approval for the neuroimaging data from Chongqing Medical School do not permit public archiving of those individual anonymised MRI data. Readers seeking information about those data should contact the author Dr. Wei Cheng at the Institute of Science and Technology for Brain-inspired Intelligence, Fudan University, Shanghai, 200433, PR China. Email: wcheng@fudan.edu.cn. Specifically, requestors must meet the following conditions to obtain the data: completion of a formal data sharing agreement. The code used in the study used standard functions available in Matlab™ and SPM, and is archived at https://osf.io/zbqn7/. J.F. is also supported by Shanghai Municipal Science and Technology Major Project (No.2018SHZDZX01) and ZJLab.

Declaration of Competing Interest

None of the authors declares a conflict of interest.

CRediT authorship contribution statement

Jingnan Du: Conceptualization, Data curation, Formal analysis, Investigation, Methodology, Software, Validation, Visualization, Writing - review & editing. **Edmund T. Rolls:** Conceptualization, Methodology, Software, Formal analysis, Investigation, Writing - original draft, Writing - review & editing, Visualization. **Wei Cheng:** Conceptualization, Data curation, Formal analysis, Funding acquisition, Investigation, Methodology, Project administration, Resources, Software, Supervision, Validation, Visualization, Writing - review & editing. **Yu Li:** Data curation, Funding acquisition, Investigation, Methodology, Project administration, Resources, Writing - review & editing. **Weikang Gong:** Data curation, Formal analysis. **Jiang Qiu:** Data curation, Funding acquisition, Investigation, Methodology, Project administration, Resources, Writing - review & editing. **Jianfeng Feng:** Funding acquisition, Project administration, Resources, Supervision.

Acknowledgements

The use of resting state fMRI data from the Nathan Kline Institute–Rockland Sample (NKI-RS) dataset (Nooner et al., 2012) is gratefully acknowledged.

Supplementary data

Supplementary data to this article can be found online at https://doi.org/10.1016/j.cortex.2019.10.012.

REFERENCES

Amunts, K., & Zilles, K. (2012). Architecture and organizational principles of Broca's region. *Trends in Cognitive Sciences, 16*(8), 418–426. https://doi.org/10.1016/j.tics.2012.06.005.

Aron, A. R., Robbins, T. W., & Poldrack, R. A. (2014). Inhibition and the right inferior frontal cortex: One decade on. *Trends in Cognitive Sciences, 18*(4), 177–185. https://doi.org/10.1016/j.tics.2013.12.003.

Brodmann, K. (1909a). *Localisation in the cerebral cortex (L. J. Garey, trans.)*. London: Imperial College Press, 1999.

Brodmann, K. (1909b). *Vergleichende Lokalisationslehre der Grosshirnrinde in ihren Prinzipien dargestellt auf Grund des Zellenbaues*. Leipzig: Barth.

Cabral, J., Kringelbach, M. L., & Deco, G. (2014). Exploring the network dynamics underlying brain activity during rest. *Progress in Neurobiology, 114*, 102–131. https://doi.org/10.1016/j.pneurobio.2013.12.005.

Carmichael, S. T., & Price, J. L. (1996). Connectional networks within the orbital and medial prefrontal cortex of macaque monkeys. *Journal of Comparative Neurology, 371*, 179–207.

Chao-Gan, Y., & Yu-Feng, Z. (2010). DPARSF: A MATLAB toolbox for "pipeline" data analysis of resting-state fMRI. *Frontiers in Systems Neuroscience, 4*, 13.

Cheng, W., Rolls, E. T., Qiu, J., Liu, W., Tang, Y., Huang, C. C., et al. (2016). Medial reward and lateral non-reward orbitofrontal cortex circuits change in opposite directions in depression. *Brain, 139*(Pt 12), 3296–3309. https://doi.org/10.1093/brain/aww255.

Cheng, W., Rolls, E. T., Qiu, J., Xie, X., Lyu, W., Li, Y., et al. (2018). Functional connectivity of the human amygdala in health and in depression. *Social Cognitive and Affective Neuroscience, 13*(6), 557–568. https://doi.org/10.1093/scan/nsy032.

Cheng, W., Rolls, E. T., Qiu, J., Xie, X., Wei, D., Huang, C. C., et al. (2018). Increased functional connectivity of the posterior cingulate cortex with the lateral orbitofrontal cortex in depression. *Translational Psychiatry, 8*(1), 90. https://doi.org/10.1038/s41398-018-0139-1.

Cheng, W., Rolls, E. T., Qiu, J., Yang, D., Ruan, H., Wei, D., et al. (2018). Functional connectivity of the precuneus in unmedicated patients with depression. *Biology Psychiatry Cognitive Neuroscience Neuroimaging, 3*(12), 1040–1049. https://doi.org/10.1016/j.bpsc.2018.07.008.

Cheng, W., Rolls, E. T., Ruan, H., & Feng, J. (2018). Functional connectivities in the brain that mediate the association between depressive problems and sleep quality. *JAMA Psychiatry, 75*, 1052–1061.

Clos, M., Amunts, K., Laird, A. R., Fox, P. T., & Eickhoff, S. B. (2013). Tackling the multifunctional nature of Broca's region meta-analytically: Co-activation-based parcellation of area 44. *NeuroImage, 83*, 174–188. https://doi.org/10.1016/j.neuroimage.2013.06.041.

de Araujo, I. E. T., Rolls, E. T., Velazco, M. I., Margot, C., & Cayeux, I. (2005). Cognitive modulation of olfactory processing. *Neuron, 46*, 671–679.

Deco, G., Rolls, E. T., Albantakis, L., & Romo, R. (2013). Brain mechanisms for perceptual and reward-related decision-making. *Progress in Neurobiology, 103*, 194–213.

Deng, W. L., Rolls, E. T., Ji, X., Robbins, T. W., Banaschewski, T., Bokde, A. L. W., et al. (2017). Separate neural systems for behavioral change and for emotional responses to failure during behavioral inhibition. *Human Brain Mapping, 38*, 3527–3537.

Faisal, A. A., Selen, L. P., & Wolpert, D. M. (2008). Noise in the nervous system. *Nature Reviews Neuroscience, 9*(4), 292–303.

Friston, K. J., Williams, S., Howard, R., Frackowiak, R. S., & Turner, R. (1996). Movement-related effects in fMRI time-series. *Magnetic Resonance in Medicine, 35*(3), 346–355.

Grabenhorst, F., D'Souza, A., Parris, B. A., Rolls, E. T., & Passingham, R. E. (2010). A common neural scale for the subjective pleasantness of different primary rewards. *NeuroImage, 51*, 1265–1274.

Grabenhorst, F., & Rolls, E. T. (2011). Value, pleasure, and choice in the ventral prefrontal cortex. *Trends in Cognitive Sciences, 15*, 56–67.

Grabenhorst, F., Rolls, E. T., & Bilderbeck, A. (2008). How cognition modulates affective responses to taste and flavor: Top down influences on the orbitofrontal and pregenual cingulate cortices. *Cerebral Cortex, 18*, 1549–1559.

Grabenhorst, F., Rolls, E. T., & Parris, B. A. (2008). From affective value to decision-making in the prefrontal cortex. *European Journal of Neuroscience, 28*, 1930–1939.

Grabenhorst, F., Rolls, E. T., Parris, B. A., & D'Souza, A. (2010). How the brain represents the reward value of fat in the mouth. *Cerebral Cortex, 20*, 1082–1091.

Henssen, A., Zilles, K., Palomero-Gallagher, N., Schleicher, A., Mohlberg, H., Gerboga, F., et al. (2016). Cytoarchitecture and probability maps of the human medial orbitofrontal cortex. *Cortex, 75*, 87–112. https://doi.org/10.1016/j.cortex.2015.11.006.

Kahnt, T., Chang, L. J., Park, S. Q., Heinzle, J., & Haynes, J. D. (2012). Connectivity-based parcellation of the human orbitofrontal cortex. *The Journal of Neuroscience, 32*(18), 6240–6250. https://doi.org/10.1523/JNEUROSCI.0257-12.2012.

Kringelbach, M. L., & Rolls, E. T. (2003). Neural correlates of rapid reversal learning in a simple model of human social interaction. *NeuroImage, 20*, 1371–1383.

Nooner, K. B., Colcombe, S. J., Tobe, R. H., Mennes, M., Benedict, M. M., Moreno, A. L., et al. (2012). The NKI-Rockland sample: A model for accelerating the pace of discovery science in psychiatry. *Frontiers in Neuroscience, 6*, 152. https://doi.org/10.3389/fnins.2012.00152.

O'Doherty, J., Kringelbach, M. L., Rolls, E. T., Hornak, J., & Andrews, C. (2001). Abstract reward and punishment representations in the human orbitofrontal cortex. *Nature Neuroscience, 4*, 95–102.

Öngür, D., Ferry, A. T., & Price, J. L. (2003). Architectonic division of the human orbital and medial prefrontal cortex. *Journal of Comparative Neurology, 460*, 425–449.

Ongür, D., & Price, J. L. (2000). The organisation of networks within the orbital and medial prefrontal cortex of rats, monkeys and humans. *Cerebral Cortex, 10*, 206–219.

Power, J. D., Mitra, A., Laumann, T. O., Snyder, A. Z., Schlaggar, B. L., & Petersen, S. E. (2014). Methods to detect, characterize, and remove motion artifact in resting state fMRI. *NeuroImage, 84*, 320–341. https://doi.org/10.1016/j.neuroimage.2013.08.048.

Price, J. L. (1999). Networks within the orbital and medial prefrontal cortex. *Neurocase, 5*, 231–241.

Price, J. L. (2006). Connections of orbital cortex. In D. H. Zald, & S. L. Rauch (Eds.), *The orbitofrontal cortex* (pp. 39–55). Oxford: Oxford University Press.

Price, J. L. (2007). Definition of the orbital cortex in relation to specific connections with limbic and visceral structures and other cortical regions. *Annals of the New York Academy of Sciences, 1121*, 54–71.

Rolls, E. T. (2014). *Emotion and decision-making explained*. Oxford: Oxford University Press.

Rolls, E. T. (2016a). *Cerebral cortex: Principles of operation*. Oxford: Oxford University Press.

Rolls, E. T. (2016b). Functions of the anterior insula in taste, autonomic, and related functions. *Brain and Cognition, 110*, 4–19.

Rolls, E. T. (2016c). A non-reward attractor theory of depression. *Neuroscience and Biobehavioral Reviews, 68*, 47–58. https://doi.org/10.1016/j.neubiorev.2016.05.007.

Rolls, E. T. (2018). *The brain, emotion, and depression*. Oxford: Oxford University Press.

Rolls, E. T. (2019a). The cingulate cortex and limbic systems for action, emotion, and memory. In B. A. Vogt (Ed.), *Handbook of clinical neurology: Cingulate cortex*. New York: Elsevier.

Rolls, E. T. (2019b). The cingulate cortex and limbic systems for emotion, action, and memory. *Brain Structure & Function, 224*, 3001–3018. https://doi.org/10.1007/s00429-019-01945-2.

Rolls, E. T. (2019c). *The orbitofrontal cortex*. Oxford: Oxford University Press.

Rolls, E. T. (2019d). The orbitofrontal cortex and emotion in health and disease, including depression. *Neuropsychologia, 128*, 14–43. https://doi.org/10.1016/j.neuropsychologia.2017.09.021.

Rolls, E. T., Cheng, W., Du, J., Wei, D., Qiu, J., Dai, D., et al. (2019). *Functional connectivity of the right inferior frontal gyrus and orbitofrontal cortex in depression* (submitted for publication).

Rolls, E. T., Cheng, W., & Feng, J. (2019). *The orbitofrontal cortex: A key brain region in depression* (submitted for publication).

Rolls, E. T., Cheng, W., Gong, W., Qiu, J., Zhou, C., Zhang, J., et al. (2019). Functional connectivity of the anterior cingulate cortex in depression and in health. *Cerebral Cortex, 29*, 3617–3630. https://doi.org/10.1093/cercor/bhy236.

Rolls, E. T., & Deco, G. (2010). *The noisy brain: Stochastic dynamics as a principle of brain function*. Oxford: Oxford University Press.

Rolls, E. T., Huang, C. C., Lin, C. P., Feng, J., & Joliot, M. (2019). Automated anatomical labelling atlas 3. *NeuroImage*, 116189. https://doi.org/10.1016/j.neuroimage.2019.116189.

Rolls, E. T., Joliot, M., & Tzourio-Mazoyer, N. (2015). Implementation of a new parcellation of the orbitofrontal cortex in the automated anatomical labeling atlas. *Neuroimage, 122*, 1–5. https://doi.org/10.1016/j.neuroimage.2015.07.075.

Rolls, E. T., Kringelbach, M. L., & de Araujo, I. E. T. (2003). Different representations of pleasant and unpleasant odors in the human brain. *European Journal of Neuroscience, 18*, 695–703.

Rushworth, M. F., Kolling, N., Sallet, J., & Mars, R. B. (2012). Valuation and decision-making in frontal cortex: One or many serial or parallel systems? *Current Opinion in Neurobiology, 22*(6), 946–955. https://doi.org/10.1016/j.conb.2012.04.011.

Van Essen, D. C., Hayashi, T., Autio, J., Ose, T., Nishigori, K., Coalsor, T., et al. (2019). Evaluation of functional connectivity using retrograde tracers in the macaque monkey. *Organisation for Human Brain Mapping*. https://ww5.aievolution/hmb1901.

Vogt, B. A. (Ed.). (2009). *Cingulate neurobiology and disease*. Oxford: Oxford University Press.

Xie, C., Jia, T., Rolls, E. T., Liu, Z., Banaschewski, T., Barker, G., et al. (2019). *Reward vs non-reward sensitivity of the medial vs lateral orbitofrontal cortex related to depression* (submitted for publication).

y Cajal, S. R. (1995). *Histology of the nervous system of man and vertebrates* (Vol. 1). USA: Oxford University Press.